14 August 1998

ELSEVIER

Chemical Physics Letters 292 (1998) 651–655

CHEMICAL PHYSICS LETTERS

Photoelectron spectroscopy of CH_3O^- and CD_3O^-

David L. Osborn [a,b,1], David J. Leahy [a,b,2], Eun Ha Kim [a,b], Esther de Beer [a,b,3], Daniel M. Neumark [a,b,*]

[a] *Department of Chemistry, University of California, Berkeley, CA 94720, USA*
[b] *Chemical Sciences Division, Lawrence Berkeley National Laboratory, Berkeley, CA 94720, USA*

Received 30 March 1998; in final form 12 June 1998

Abstract

The photoelectron spectra of the methoxide anions, CH_3O^- and CD_3O^-, have been measured at 8–10 meV resolution. The spectra show resolved vibrational structure corresponding to vibrational levels of the $CH_3O/CD_3O\,\tilde{X}(^2E)$ state. These vibrational progressions are assigned to the degenerate ν_5 and ν_6 modes of the methoxy radical; no progressions in the totally symmetric stretch modes are observed. In addition, we obtain refined electron affinities: $EA(CH_3O) = 1.568 \pm 0.005$ and $EA(CD_3O) = 1.551 \pm 0.005$ eV.

1. Introduction

More than 40 years after its initial detection [1], the methoxy radical remains a challenging and fruitful subject of molecular spectroscopy. The $\tilde{X}(^2E)$ ground electronic state of CH_3O, within C_{3v} symmetry, is orbitally degenerate with an unpaired electron spin, leading to complications arising from Jahn–Teller (JT) and spin–orbit interactions. The complexity of the ground-state vibronic structure is evident from numerous investigations using dispersed fluorescence [2–5] (DF) and rotationally resolved stimulated emission pumping (SEP) [6–9]; these have resulted in clear assignments of most ground-state frequencies, but conflicting assignments for the degenerate (JT-active) vibrational modes. In this letter we report photoelectron spectra of two methoxide anion isotopomers, CH_3O^- and CD_3O^-; these data provide an independent route for the study of the CH_3O ground-state vibrational frequencies.

Reed and Brauman [10] measured the photodestruction of methoxide trapped in an ion cyclotron resonance cell as a function of excitation energy, obtaining an electron affinity (EA) of 1.59 ± 0.04 eV from the threshold for this process. Engelking et al. [11] measured the photoelectron spectrum of both CH_3O^- and CD_3O^- directly using a fixed-frequency hemispherical analyzer photoelectron spectrometer. This spectrum yielded a more precise determination of $EA(CH_3O)$, 1.570 ± 0.022 eV, and isotopic substitution definitively established the carrier of the signal as CH_3O^-, rather than CH_2OH^-. With an electron kinetic energy (e_{KE}) resolution of 60 meV, their spectrum showed evidence of a single vibra-

* Corresponding author.
E-mail: dan@radon.cchem.berkeley.edu
[1] Current address: JILA, Campus Box 440, Boulder, CO 80309-0440, USA.
[2] Current address: World's Inc., 520 Third Street, Suite 201, San Francisco, CA 94107, USA.
[3] Current address: Philips Research Laboratories, Eindhoven, The Netherlands.

0009-2614/98/$19.00
PII: S0009-2614(98)00717-9

tional progression in the neutral which they assigned to the totally symmetric ν_2 umbrella mode with a frequency of 1325 ± 30 cm^{-1}. A somewhat higher resolution (~ 30 meV) photoelectron spectrum of CD_3O^- was reported by Oakes et al. [12] without further interpretation. Here we report the photoelectron spectrum of both isotopomers at 8–10 meV resolution; these results along with spectra of similar quality obtained in other laboratories [13,14] suggest a re-interpretation of the vibrational features in the spectrum.

2. Experimental

The photoelectron spectra of methoxide anions were recorded on our time-of-flight negative ion photoelectron spectrometer. The apparatus has been described in detail elsewhere [15], but a brief description is given here. Methoxide ions are formed in an electric discharge [16] during a pulsed supersonic expansion of CH_3OH (CD_3OD) seeded in 5 atm Ne. Cold ions are extracted perpendicularly into a Wiley–McLaren [17] time-of-flight mass spectrometer at an energy of 1 keV, separated according to mass, and detected via a microchannel plate detector. Ions of mass 31 are selectively photodetached by the second harmonic of a Nd:YAG laser (532 nm), or by 416 nm light generated by Raman-shifting a 355 nm laser pulse in a high-pressure H_2 Raman cell. The kinetic energy distribution of the photoelectrons is determined by measuring their time-of-flight through a 1 m field-free region perpendicular to the laser and ion beam directions. In addition, the laser polarization angle can be rotated to investigate photoelectron angular distributions. The instrumental resolution is 8–10 MeV for 0.65 eV electrons and degrades as $(e_{KE})^{3/2}$. The low-energy cutoff for electron detection occurs at ≈ 0.25 eV.

3. Results and discussion

The CH_3O^- photoelectron spectra taken at 532 and 416 nm are shown in Fig. 1a,b, respectively. The spectrum at 416 nm was taken at two laser polarization angles, $\theta = 0°$ and 90°, defined with respect to the electron detection axis. The experimental observable is the electron kinetic energy (e_{KE}), related to the molecular energy levels by

$$e_{KE} = h\nu - EA - E_\nu^{(0)} + E_\nu^{(-)} \quad (1)$$

where $h\nu$ is the photon energy, EA is the electron affinity of CH_3O, and $E_\nu^{(0)}$ and $E_\nu^{(-)}$ are the vibrational energies of the anion and neutral, respectively. The x-axes of the spectra in Fig. 1 shows the electron binding energy (e_{BE}), given by

$$e_{BE} = h\nu - e_{KE}\,. \quad (2)$$

The structure in the spectra represent transitions to various vibrational levels of the $CH_3O\,\tilde{X}(^2E)$ state. Peak 'a' is assigned to the 0_0^0 origin transition, yielding $EA(CH_3O) = 1.568 \pm 0.005$ eV, in good agreement with Engelking et al. [11]. Essentially all the ions are in their zero-point level as evidenced by the absence of hot-bands to lower e_{BE} of the origin transition. Due to lower electron detection efficiency for $e_{KE} < 0.25$ eV ($e_{BE} > 2.08$ eV at 532 nm), the

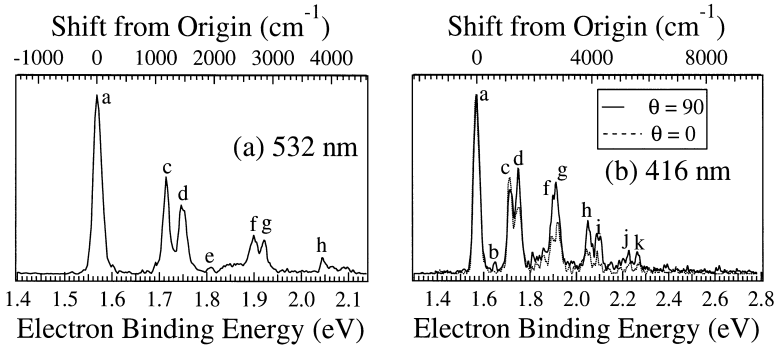

Fig. 1. Photoelectron spectra of CH_3O^- acquired (a) at 532 nm with laser polarization parallel ($\theta = 0°$) to the ion beam axis and (b) at 416 nm with both polarization directions.

Table 1
CH_3O vibrational assignments and energies for transitions in Fig. 1

Peak	Binding energy (eV)	Shift from origin (cm^{-1})	SEP frequency[a] (cm^{-1})	Assignment	
a	1.568	0	–	0_0^0	
b	1.651	669	652	6_0^1	$j = 3/2$
c	1.714	1178	1198	6_0^1	$j = 1/2$
d	1.749	1460	1489	5_0^1	$j = 1/2$
e	1.809	1944	1966	$5_0^1 6_0^1$	$j = 1/2$
f	1.899	2670	–	$5_0^1 6_0^1$	$j = 5/2$?
g	1.921	2847	–	–	
h	2.049	3875	–	–	
i	2.099	4283	–	–	
j	2.231	5347	–	–	
k	2.269	5654	–	–	

[a] Refs. [6,7].

structure appears to end at peak *h* in Fig. 1a. Increasing the photon energy to 416 nm (Fig. 1b) shows additional vibrational features. Positions and spacings of the observed CH_3O peaks are given in Table 1. A corresponding photoelectron spectrum of CD_3O^- at 416 nm is presented in Fig. 2, with relevant peak positions listed in Table 2. The electron affinity measured from this spectrum, $EA(CD_3O) = 1.551 \pm 0.005$ eV, is in good agreement with previous determinations of 1.552 ± 0.022 [11] and 1.551 ± 0.007 eV [12].

Photodetachment to the ground state of CH_3O results involves ejection of an electron from the fully occupied (2e) [4] orbital of CH_3O^-, a non-bonding p-type orbital localized on the oxygen atom. This is consistent with the origin appearing as the strongest peak in the spectrum, implying a relatively small geometry change from anion to neutral.

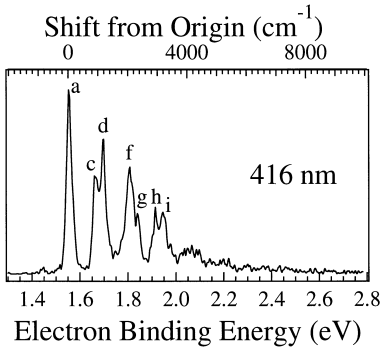

Fig. 2. Photoelectron spectrum of CD_3O^- acquired at 416 nm with vertical polarization ($\theta = 90°$). Peak labels match the corresponding vibronic transitions for CH_3O in Fig. 1.

Methoxy has six vibrational modes: the singly degenerate ν_1, ν_2, and ν_3 modes of a_1-symmetry, and the doubly degenerate ν_4, ν_5, and ν_6 modes of e-symmetry. Under normal circumstances, only the totally symmetric vibrational modes are active in the photoelectron spectrum. The ν_1 symmetric C–H stretch will certainly have a frequency greater than 2000 cm^{-1} ($\nu_1 = 2965$ cm^{-1} in CH_3F) [19] and cannot plausibly give rise to peaks b–d. Similarly, the fundamental (1046 cm^{-1}) and first overtone (2074 cm^{-1}) frequencies of the ν_3 C–O stretching mode are well established from DF [2–5] and SEP experiments [6–9] on the $CH_3O\tilde{A}(^2A_1) \rightarrow \tilde{X}(^2E)$ transition, and cannot explain any of the peaks in Fig. 1. The frequency of the only remaining a_1-vibration, the ν_2 umbrella mode (1360 cm^{-1}), is also well-known, and could reasonably represent the progression in the photoelectron spectrum under lower resolution such that the c/d, f/g, etc., splittings are not resolved, as was previously the case [11]. However, the present spectrum renders this assignment unsatisfactory. At most the ν_2 progression is only weakly active, with its fundamental obscured between peaks ‘c’ and ‘d’.

By a process of elimination we are left with an unusual situation in which all prominent vibrational structure in Fig. 1 must be assigned to e-symmetry modes. The fact that single excitations in these de-

Table 2
CD_3O vibrational assignments and energies for transitions in Fig. 2

Peak	Binding energy (eV)	Shift from origin (cm^{-1})	SEP frequency[a] (cm^{-1})	Assignment	
a	1.551	0	–	0_0^0	
b	–	–	–	–	
c	1.664	911	885	6_0^1	$j = 1/2$
d	1.696	1170	1172	5_0^1	$j = 1/2$
e	–	–	–	–	
f	1.805	2049	–	$5_0^1 6_0^1$	$j = 5/2$?
g	1.840	2331	–	–	
h	1.914	2928	–	–	
i	1.946	3186	–	–	

[a]Ref. [18].

generate modes are observed in CH_3O can be ascribed to JT coupling of vibrational and electronic motion in the $\tilde{X}$ state [20]. If a single quantum in a degenerate vibration is excited in a ^2E electronic state, the vibrational angular momentum l and the projection of the orbital angular momentum along the C_{3v} symmetry axis Λ take on the values $l = 1$, and $\Lambda = 1$. A linear JT interaction splits this 4-fold degenerate vibronic level into two doubly degenerate levels, one of A_1/A_2 vibronic symmetry, and a second of E-vibronic symmetry. The JT quantum number $j \equiv l \pm 1/2\,\Lambda$ takes the values $j = 3/2$ for A_1/A_2 levels, and $j = 1/2$ for E-levels. The addition of a quadratic JT interaction further splits the A_1/A_2 levels, while the E-level remains degenerate for all strengths of vibronic interaction.

If only linear JT coupling is present, the optical selection rule for a transition between a non-degenerate and degenerate electronic state is $l' = j \pm 1/2$, where l' is the vibrational angular momentum of the level associated with the non-degenerate electronic state [20]. This selection rule is relaxed for non-zero quadratic JT coupling. Similar rules apply in photoelectron spectroscopy. Thus, transitions from the ground vibrational state ($l' = 0$) of CH_3O^- to levels of the CH_3O $\tilde{X}(^2E)$ state with $j = 1/2$ will be the strongest JT-allowed transitions, with weaker transitions to $j = 3/2$ levels also possible from quadratic JT coupling.

With these considerations in mind, features in the CH_3O^- photoelectron spectrum can be assigned by comparison of our spectrum with the results of Temps and coworkers [8,9], who have used rotationally resolved SEP spectroscopy and dispersed fluorescence to assign frequencies for all the JT components of the 6^1 and 5^1 vibrational levels in the $\tilde{X}$ state (see Table 1). Their frequencies for the $j = 3/2(A_1)$ and $j = 1/2(E)$ components of the 6^1 level are in good agreement with peaks 'b' and 'c', respectively, in the photoelectron spectrum of Fig. 1. Similarly, peak 'd' can be assigned as the $j = 1/2$, E-symmetry component of the 5^1 level. Peaks 'c' and 'd' are much more intense than peak 'b', consistent with the linear JT selection rule. Our assignments in Table 1 are supported by the observation that the intensities of peaks 'b' and 'c' in Fig. 1b show opposite dependence on laser polarization angle, consistent with differing vibronic symmetries (A_1 vs. E, respectively) of the neutral levels. Note, however, that peaks 'c' and 'd' exhibit somewhat different polarization dependences even though they are both transitions to $j = 1/2(E)$ levels.

The remaining peaks (e–k) most likely arise from overtones of ν_5 and ν_6 along with combination bands between these modes. However, neither harmonic nor Morse potentials provide a satisfactory fit to these features based on the fundamental frequencies assigned above. This is perhaps not too surprising in light of the complicated vibronic energy level structures that can arise when there are two JT-active modes [21].

Although too small to be resolved in our apparatus, the 62 cm^{-1} spin–orbit splitting of the $CH_3O\,\tilde{X}(^2E)$ state [2] contributes to the 160 cm^{-1} width of the origin transition, peak 'a'; the other contributing factors are rotational excitation in the anion and the instrument response function. In contrast, the 6_0^1 transition, peak 'c', has a width of only

113 cm^{-1}. We attribute the majority of the decrease in linewidth to quenching of spin–orbit splitting due to excitation of an e-vibration in this JT-perturbed electronic state. This interpretation agrees with dispersed fluorescence spectra [2] of the $CH_3O\,\tilde{A}(^2A_1) \rightarrow \tilde{X}(^2E)$ transition, which also show no spin–orbit splitting in levels of the $\tilde{X}$ state for which vibrational modes of e-symmetry are excited.

The isotopomer CD_3O [2,3,22,18] has not been studied as extensively as CH_3O. The peaks in the CD_3O^- photoelectron spectrum show a pattern very similar to the CD_3O^- spectrum, leading by comparison to the assignments given in Table 2. The CH_3O/CD_3O $\tilde{X}(^2E)$ frequency ratios for corresponding peaks range from 1.25 to 1.30. This substantial isotope shift is further evidence that the totally symmetric ν_3 C–O stretching mode, which contains essentially no hydrogen atom motion, is not active in the spectrum of either isotopomer. The ν_5 and ν_6 modes, on the other hand, are both described by significant hydrogen motion, consistent with the present vibrational assignments. In contrast to the $\theta = 90°$ 416 nm CH_3O^- spectrum in Fig. 1b, there is no evidence for peak 'b', the 6^1 $j = 3/2(A_1)$ level, in the $\theta = 90°$ CD_3O^- spectrum (not shown). This peak is expected to have low intensity, and is probably obscured in the wings of peaks 'a' and 'c', which are more closely spaced in CD_3O than in CH_3O. The comparison between normal and deuterated vibronic energy spacings will be a useful constraint in further theoretical calculations on the JT effect in methoxy.

In conclusion, we have shown that the photoelectron spectra of CH_3O^- and CD_3O^- are significantly more complex than the previously published spectra [11] suggest. We propose that the main progressions in the photoelectron spectrum arise from nominally forbidden (but Jahn–Teller allowed) excitations in the e-symmetry modes ν_5 and ν_6. The greater strength of transitions to $j = 1/2$ levels compared to $j = 3/2$ levels suggests a greater importance for the linear as opposed to quadratic JT interaction terms.

Acknowledgements

This research is supported by the Air Force Office of Scientific Research under Grant. No. F49620-97-1-0018. We thank Professor F. Temps for providing vibrational frequency data prior to publication, and Professors W.C. Lineberger and G.B. Ellison for helpful discussions. DLO is a NDSEG Predoctoral fellow.

References

[1] D.W.G. Style, J.C. Ward, Trans. Faraday Soc. 49 (1953) 999.
[2] G. Inoue, H. Akimoto, M. Okuda, J. Chem. Phys. 72 (1980) 1769.
[3] S.C. Foster, P. Misra, T.D. Lin, C.P. Damo, C.C. Carter, T.A. Miller, J. Phys. Chem. 92 (1988) 5914.
[4] Y.-Y. Lee, G.-H. Wann, Y.P. Lee, J. Chem. Phys. 99 (1993) 9465.
[5] P. Misra, H. Hzu, C.-Y. Hsueh, J.B. Halpern, Chem. Phys. 178 (1993) 377.
[6] A. Geers, J. Kappert, F. Temps, T.J. Sears, J. Chem. Phys. 98 (1993) 4297.
[7] A. Geers, J. Kappert, F. Temps, J.W. Wiebrecht, J. Chem. Phys. 101 (1994) 3618.
[8] F. Temps, in: H.L. Dai, R.W. Field (Eds.), Molecular Spectroscopy and Dynamics by Stimulated Emission Pumping, World Scientific, Singapore, 1995, p. 375.
[9] A. Geers, J. Kappert, C. Stock, C. Wedel, F. Temps, J. Phys. Chem., to be published.
[10] K.J. Reed, J.I. Brauman, J. Am. Chem. Soc. 97 (1975) 1625.
[11] P.C. Engelking, G.B. Ellison, W.C. Lineberger, J. Chem. Phys. 69 (1978) 1826.
[12] J.M. Oakes, L.B. Harding, G.B. Ellison, J. Chem. Phys. 83 (1985) 5400.
[13] S. Casey, D.G. Leopold, private communication
[14] K. Murray, W.C. Lineberger, private communication.
[15] R.B. Metz, A. Weaver, S.E. Bradforth, T.N. Kitsopoulos, D.M. Neumark, J. Phys. Chem. 94 (1990) 1377.
[16] D.L. Osborn, D.J. Leahy, D.R. Cyr, D.M. Neumark, J. Chem. Phys. 104 (1996) 5026.
[17] W.C. Wiley, I.H. McLaren, Rev. Sci. Instrum. 26 (1955) 1150.
[18] A. Geers, J. Kappert, S. Stöck, F. Temps, J.W. Wiebrecht, Nachrichten der Adademie der Wissenschaften in Göttingen II. Mathematisch-Physikalische Klasse, No. 2, Vandenhoeck and Ruprecht, Göttingen, 1993.
[19] G. Herzberg, Molecular Spectra and Molecular Structure. II: Infrared and Raman Spectra of Polyatomic Molecules, Van Nostrand Reinhold, New York, 1945, pp. 315.
[20] H.C. Longuet-Higgins, U. Öpik, M.H.L. Pryce, R.A. Sack, Proc. Roy. Soc. 244A (1958) 1.
[21] H. Koppel, W. Domcke, L.S. Cederbaum, Adv. Chem. Phys. 57 (1984) 59.
[22] S.D. Brossard, P.G. Carrick, E.L. Chappell, S.C. Hulegaard, P.C. Engelking, J. Chem. Phys. 84 (1986) 2459.